Direct Observation of Friedel Oscillations around Incorporated Si_{Ga} Dopants in GaAs by Low-Temperature Scanning Tunneling Microscopy

M. C. M. M. van der Wielen, A. J. A. van Roij, and H. van Kempen
Research Institute for Materials, University of Nijmegen, Toernooiveld 1, 6525 ED Nijmegen, The Netherlands
(Received 25 July 1995)

We report the direct imaging of electrically active Si dopants near the GaAs(110) surface with a scanning tunneling microscope at a temperature of 4.2 K. In the filled state images, we observe patterns of rings which are centered around the individual doping atoms. We believe these ring patterns are induced by the individual impurities, which, due to their charge, disturb the local potential and cause oscillations in the charge density, also called Friedel oscillations. In the empty state images no Friedel oscillations can be observed.

PACS numbers: 61.16.Ch, 68.35.Dv, 71.55.Eq, 73.20.Hb

Recently, two groups reported the direct imaging of individual dopants in the subsurface region of the GaAs(110) surface with a scanning tunneling microscope (STM) [1–3]. Johnson *et al.* [1] showed that Zn dopants (Zn_{Ga}) and Be dopants (Be_{Ga}) in the top five subsurface layers influence the GaAs(110) surface electronic structure. Zheng *et al.* [2] obtained similar results for substitutional Si dopants (Si_{Ga}). They showed that at both bias polarities individual dopants (Si_{Ga} and Zn_{Ga}) induce hillock features in the STM images superimposed on the atomic sublattice. The local increase in conductance is explained by the presence of a Coulomb potential around the charged doping atoms. All these results were obtained under UHV conditions at room temperature.

In this paper we report on STM measurements of the GaAs(110) surface at a temperature of 4.2 K. We will show first STM images of individual Si dopants near the GaAs(110) surface measured at low temperature. Since the STM is cooled down more than 85 °C below the boiling point of oxygen, the vapor pressure of oxygen is extremely low ($< 10^{-15}$ Torr). Therefore surfaces like GaAs(110) and AlGaAs(110), which normally oxidize very quickly, will stay clean under these conditions for many days. Cleaving these samples *in situ* at a temperature of 4.2 K, therefore, gives us the potential of studying clean surfaces with atomic resolution. In addition, we obtain a high spectral resolution ($k_BT \approx 0.4$ meV). In this way we foresee the possibility of doing high-resolution local spectroscopy measurements on different kinds of III-V semiconductor materials including molecular-beam-epitaxy-grown multilayer structures.

In this Letter, we show STM images of features induced by individual Si dopants measured at different bias voltages at both polarities. At positive sample bias, hillocks are visible superimposed on the Ga sublattice. At negative sample bias, we obtain a totally different picture. Patterns of black and white rings are visible around each impurity. These ring patterns we attribute to oscillations in the charge density, also known as Friedel oscillations [4]. This is not the first time Friedel oscillations have been observed with STM. Earlier experiments performed on metal and graphite surfaces show oscillations in the charge density in the vicinity of step edges [5,6], adsorbates [7], and defects [8,9]. Disturbances in the local potential are caused by irregularities in the surface geometry, in this case. As far as we know, our experiments show first observations of Friedel oscillations around individual impurities incorporated in the subsurface region. This allows the study of charge density oscillations in three dimensions by looking at impurities positioned in different subsurface layers.

In this Letter we will only show constant current images. Since the contribution to the tunneling current is dominant for electrons coming from the Fermi level, our images will show charge density oscillations which exist at the Fermi surface. We show that the Fermi energy, which can be directly derived from the oscillation period in a scan image, is comparable to a value obtained from calculations on the surface electrostatic potential. The calculation is done for a one-dimensional tunnel junction, where tip-induced band bending is included. Furthermore, we see that the period of the oscillations reduces with increasing bias voltage. This we can explain by tip-induced band bending following the one-dimensional model.

All the experiments are performed in a low-temperature STM. The STM is described in detail by Wildöer *et al.* [10]. For our experiments we equipped the STM with an *in situ* sample cleaver, which can be controlled from outside the cryostat. The samples used in all the experiments come from an *n*-type Si-doped GaAs wafer with doping density 2×10^{18} cm^{-3}. According to conductivity measurements [11] the doping concentration should approximately be above 10^{17} cm^{-3} to assure conductivity at 4.2 K, necessary for STM operation. At 4.2 K, the GaAs sample is cleaved *in situ* along the (110) plane. All the measurements are done with PtIr tips, cut with scissors.

Figure 1(a) shows an STM image of the GaAs(110) surface, measured with a sample voltage of +2.0 V. Clearly

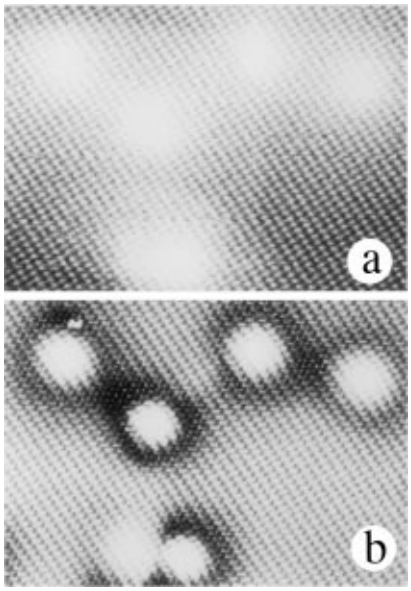

FIG. 1. Two STM images of a (110)-cleaved, $2 \times 10^{18}\,\mathrm{cm}^{-3}$ Si-doped GaAs surface. Both images are scans from the same surface area measured at opposite bias polarities. Scan size 230 Å × 165 Å. Set-point current is 100 pA. (a) Sample voltage: +2.0 V. Grey scale range: 0 to 1.1 Å. Six bright hillock features superimposed on the Ga sublattice are visible. (b) Sample voltage −2.0 V. Grey scale range 0 to 2.4 Å. At the positions of the hillock features in (a), a bright spot is visible surrounded by a black ring. These dopant-induced features are superimposed on the As sublattice.

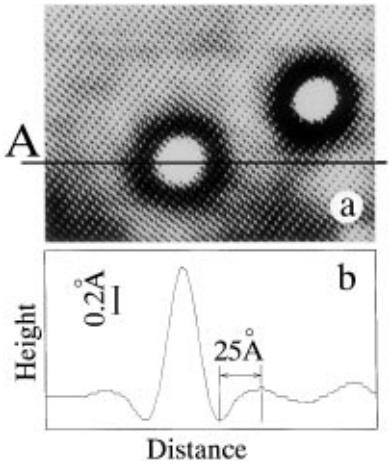

FIG. 2. (a) STM image of the (110)-cleaved, $2 \times 10^{18}\ \mathrm{cm}^{-3}$ Si-doped GaAs surface. Scan size 220 Å × 150 Å. The relative tip height is given by a grey scale, from 0 to 1.3 Å. Set-point current is 40 pA, sample voltage −2.5 V. Two dopant-induced features are displayed. Each feature consists of a bright spot in the middle, surrounded by a black ring and another white ring. The outermost ring is more pronounced in (b). (b) Cross section through the middle of the left feature along line A. The atomic lattice is filtered out. Clearly the two maxima of the outermost ring and the minima of the dark ring can be seen. From this figure we obtain an oscillation period of 50(±10) Å.

the Ga sublattice can be seen. Superimposed on the lattice bright spots are visible. These hillocks are induced by ionized Si donors present in the subsurface region [2]. From several scan images on samples with different doping concentration, we verified that the amount of features agrees with the nominal doping concentration of the material. Figure 1(b) shows an STM image of the same scan area, but this time measured with a sample voltage of −2.0 V. The bright spots turned into patterns consisting of a white spot in the middle surrounded by a black ring. The ring pattern is superimposed on the As sublattice.

Figure 2(a) shows an image with two dopant-induced features, measured with a sample voltage of −2.5 V. Next to the black ring, centered around the middle bright spot, another white ring is visible. This ring is more pronounced in Fig. 2(b), showing a cross section through the center of the left pattern as indicated by line A. In this line scan the atomic lattice is filtered out. From this picture we obtain a value of 25(±5) Å for half the oscillation period. This value we obtained by measuring the distance between the minimum of the black ring and the maximum of the outermost white ring. Notice that the size of the other feature corresponding to a doping atom positioned in another subsurface layer is somewhat smaller. The dependence between the depth of the doping atom and the observed oscillation period will be studied in a future publication [12].

We attribute the rings around the individual dopants to Friedel oscillations [4]. Friedel oscillations are oscillations in the charge density and are a direct solution of Schrödinger's equation adding a local potential variation, like a central symmetric screened Coulomb potential which is present around a charged impurity (see, for example, [13]), to the otherwise homogeneous system. Following Friedel, the oscillation period should be equal to half the electron Fermi wavelength. From Fig. 2(b) we obtain an oscillation period of 50(±10) Å, which gives an electron Fermi wavelength (λ_F) at the surface equal to 100(±20) Å. Substituting this value in the dispersion relation for free electrons, $E_F = \hbar^2 k_F^2/2m^*$ (with $k_F = 2\pi/\lambda_F$ the electron Fermi wave vector, $m^* = 0.067 m_0$ the effective electron mass), we obtain a Fermi energy (E_F) of 0.22(±0.07) eV. This value should be compared to the typical Fermi energy at the (110) surface of a Si-doped GaAs sample with doping density $2 \times 10^{18}\ \mathrm{cm}^{-3}$.

The Fermi energy in the bulk of the semiconductor can be calculated using Fermi-Dirac statistics [14]. The Fermi energy relative to the conduction band minimum for our sample is equal to +0.5 meV at a temperature of 4.2 K. The positive sign indicates that the Fermi level lies above the conduction band minimum. This sample, therefore, is degenerate. At the surface one should take into account the effect of tip-induced band bending [15]. Because of the limited amount of free carriers present in the surface region, an electric field can penetrate into the semiconductor and cause the energy bands to

bend. We calculate the electrostatic potential at the semiconductor surface versus applied voltage for a one-dimensional tunnel junction. The calculation is similar to the calculations of Feenstra and Stroscio [16]. Solving Poisson's equation by substituting the charge density for a degenerate semiconductor, we obtain the electric field at the semiconductor surface as a function of the surface electrostatic potential. Since no surface states are present in the band-gap region of the GaAs(110) surface, we are allowed to use the boundary condition $\mathbf{D}_{s,\perp} = \mathbf{D}_{v,\perp}$, between semiconductor (s) and the vacuum (v), with $\mathbf{D}$ the electric displacement vector. The potential drop across the tunnel barrier is equal to $V_b = \mathbf{E}_s \cdot \mathbf{d}$, where $\mathbf{E}_s$ is the electric field at the semiconductor surface and $\mathbf{d}$ is the tip-sample distance. The total potential drop across the tunnel barrier and semiconductor is equal to the externally applied bias plus the work-function difference between metal and semiconductor. Our calculations are done for a temperature of 4.2 K. The dopants are Si atoms (ionization energy in GaAs of 0.002 eV) with a density of 2×10^{18} cm^{-3}. Electron affinity for GaAs is 4.07 eV. For a typical tip-sample separation of 10 Å and an estimated work function of 5.5 eV for PtIr [17] we obtain, applying a sample bias of -2.5 V, a potential difference between the bulk and the GaAs surface equal to 0.28 V. Towards the surface the bands are bending downwards and the Fermi energy is positioned 0.28 eV above the bottom of the conduction band. This number is within the experimental error of the value we derived from our measurement, $0.22(\pm 0.07)$ eV.

The same calculation shows a transition around the -1.4 V sample voltage from accumulation to depletion of electrons at the surface region, when going from negative to positive sample bias. The difference between the images shown in Figs. 1(a) and 1(b) can be explained following this model. At negative sample bias, Fig. 1(b), electrons accumulate in the subsurface region and screen the charged dopants inducing oscillations in the charge density. At positive sample bias, Fig. 1(a), free electrons are depleted from the surface region. In this situation, the unscreened Coulomb potential around the ionized dopants perturbs the local density of states at the surface.

So far we showed that the oscillation period which we obtain from our STM images can be related to the electron Fermi wavelength following the expression derived by Friedel. To do so, we had to take into account the presence of tip-induced band bending. Furthermore, the influence of the tip on the local band bending explains why these oscillations can only be observed at one bias polarity. At this moment, we are not capable of giving a quantitative analysis of the complete cross sections that we measured. To explain the exact positions of the minima and maxima with respect to the central maximum we cannot simply apply the expression derived by Langer and Vosko [18] for the charge distribution around a point charge in a metal in three dimensions considering a spherically symmetric potential. These calculations are not valid for our measurements, since the physical environment in which we are studying these oscillations around individual donors has no spherical symmetry. The donor is positioned near a surface in a fast decaying electric field going into the bulk. Therefore the distribution of these oscillations around such a donor will not be spherically symmetric, but rearranged following the local potential. Moreover, with the STM we measure an off-centered cross section of the oscillations around the impurities. The period as extracted from the STM images will therefore deviate from the real oscillation period. Despite the above-mentioned complications we can do a qualitative analysis on the effect of the sample voltage on the observed ring patterns.

In Figs. 3(a)–3(d), four scans are displayed of the same dopant-induced feature measured with four different sample voltages, respectively, -1.5, -2.0, -2.5, and -3.0 V. Figure 3(e) shows cross sections through this donor from top to bottom for each of the pictures. Again, the atomic sublattice is filtered out. Our resolution was not good enough to resolve a second white ring in the feature. From this figure it is clear that the distance

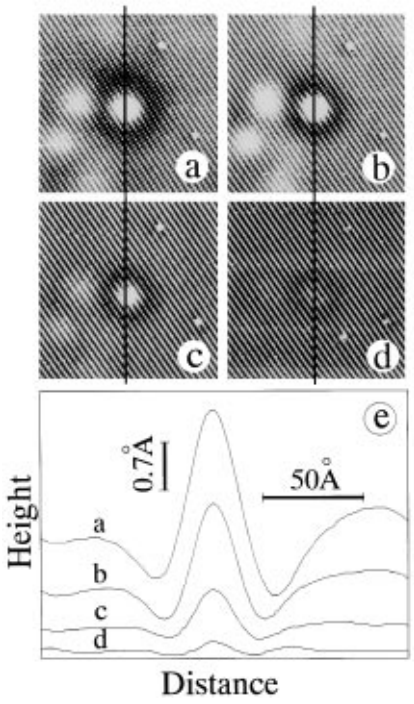

FIG. 3. Four scans are shown of the same dopant-induced feature measured with four different sample voltages, respectively, (a) -1.5, (b) -2.0, (c) -2.5, and (d) -3.0 V. Set-point current is 90 pA. Scan size 185 Å $\times$ 185 Å. The size of the pattern decreases with increasing sample voltage as is more pronounced in (e). (e) Cross sections from top to bottom through the middle of the feature for all four images as denoted by the straight lines. The atomic lattice is filtered out. The distance between the two minima is equal to 60, 49, 46, and 41 Å for a sample voltage of, respectively, -1.5, -2.0, -2.5, and -3.0 V.

between the two minima observed in each cross section decreases with increasing voltage difference between tip and sample. We obtain a distance of 60, 49, 46, and 41 Å between the minima applying a sample voltage of, respectively, -1.5, -2.0, -2.5, and -3.0 V. This behavior can be understood considering tip-induced band bending. At negative sample bias, increasing the voltage difference between tip and sample leads to an increase in the local band bending which results in a local increase of the Fermi energy and a decrease in the Fermi wavelength. Since the position of the first minimum next to the central maximum is proportional to the Fermi wavelength [18], this minimum will shift towards the middle. Notice that together with reduction of the oscillation period, when increasing the sample bias, the amplitude of the oscillations is also decreasing. This can be understood from the fact that more states below the Fermi level contribute to the tunneling current at higher bias. Therefore, the number of electrons coming from the Fermi level, with electron Fermi wave vector equal to k_F, decreases relatively to the total number of tunneling electrons and results in a less intense oscillation pattern.

In conclusion, we proved that we are capable of studying clean semiconductor surfaces at a temperature of 4.2 K with a relatively simple and inexpensive system compared to the complex UHV low-temperature systems. We have observed ring patterns in the filled state images of the clean GaAs(110) surface. These ring patterns are superimposed on the Ga sublattice, and we identified them as being caused by charge density oscillations around the substitutional Si_{Ga} dopants present in the subsurface layers. Tip-induced band bending has to be included to explain the size of the measured oscillation period and the influence of the bias voltage on the induced features.

We would like to thank E. J. G. Boon, A van Geelen, J. W. Gerritsen, J. G. H. Hermsen, R. Jansen, M. W. J. Prins, and J. W. G. Wildöer for their contribution to this work. Part of this research was supported by the Stichting Fundamenteel Onderzoek der Materie (FOM), which is financially supported by the Nederlandse Organisatie voor Wetenschappelijk Onderzoek (NWO).

[1] M. B. Johnson, O. Albrektsen, R. M. Feenstra, and H. W. M. Salemink, Appl. Phys. Lett. **63**, 2923 (1993).
[2] J. F. Zheng, X. Liu, N. Newman, E. R. Weber, D. F. Ogletree, and M. Salmeron, Phys. Rev. Lett. **72**, 1490 (1994).
[3] Z. F. Zheng, M. B. Salmeron, and E. R. Weber, Appl. Phys. Lett. **64**, 1836 (1994).
[4] J. Friedel, Nuovo Cimento **7**, 287 (1958).
[5] M. F. Crommie, C. P. Lutz, and D. M. Eigler, Nature (London) **363**, 524 (1993).
[6] Y. Hasegawa and Ph. Avouris, Phys. Rev. Lett. **71**, 1071 (1993).
[7] Ph. Avouris, I.-W. Lyo, R. E. Walkup, and Y. Hasegawa, J. Vac. Sci. Technol. B **12**, 1447 (1994).
[8] H. A. Mizes and J. S. Foster, Science **244**, 559 (1989).
[9] J. Yan, Z. Li, C. Bai, W. S. Yang, Y. Wang, W. Zhao, Y. Kang, F. C. Yu, P. Zhai, and X. Tang, J. Appl. Phys. **75**, 1390 (1994).
[10] J. W. G. Wildöer, A. J. A. van Roij, H. van Kempen, and C. J. P. M. Harmans, Rev. Sci. Instrum. **65**, 2849 (1994).
[11] O. V. Emel'yanenko, T. S. Lagunova, and D. N. Nasledov, Sov. Phys. Solid State **3**, 144 (1961).
[12] M. C. M. C. van der Wielen, A. J. A. van Roij, and H. van Kempen (to be published).
[13] J. M. Ziman, *Principles of the Theory of Solids* (Cambridge University Press, Cambridge, 1964).
[14] S. M. Sze, *Physics of Semiconductor Devices* (Wiley, New York, 1969).
[15] R. Maboudian, K. Pond, V. Bressler-Hill, M. Wassermeier, P. M. Petroff, G. A. D. Briggs, and W. H. Weinberg, Surf. Sci. Lett. **275**, L662 (1992).
[16] R. M. Feenstra and A. Stroscio, J. Vac. Sci. Technol. B **5**, 923 (1987).
[17] D. R. Lide, *CRC Handbook of Chemistry and Physics* (CRC Press, Boca Raton, 1991), 72^e edition.
[18] J. S. Langer and S. H. Vosko, J. Phys. Chem. Solids **12**, 196 (1959).